

Electrographic Response of the Heart to Myocardial Ischemia

KK Aras^{1,2,3}, S Shome⁴, DJ Swenson^{1,2,3}, J Stinstra^{2,3}, RS MacLeod^{1,2,3}

¹Bioengineering Department, University of Utah, Salt Lake City, UT, USA

²CVRTI, University of Utah, Salt Lake City, UT, USA

³SCI Institute, University of Utah, Salt Lake City, UT, USA

⁴Boston Scientific, Minneapolis, MN, USA

Abstract

Electrocardiographic (ECG) ST segment shifts are often used as markers for detecting myocardial ischemia. Literature suggests that the progression of ischemia, occurs from the endocardium and spreads towards the epicardium, eventually becoming transmural. Our study with animal models has found the progression of ischemia, characterized by ST elevations to be more complex and heterogeneous in its distribution. We used in situ canine preparations, wherein the animals were subjected to demand ischemia by reducing coronary flow and raising the heart rate through atrial pacing. At reduced flow, increasing the heart rate caused pockets of ST elevations to appear variously distributed in the sub-epicardial, mid-myocardial and endocardial regions. Further reduction in coronary flow with simultaneous raising of the heart rate, increased the extent and magnitude of ST elevated regions, that in certain cases became transmural.

1. Introduction

Myocardial ischemia is a pathological condition triggered by supply and demand imbalance of the blood to the heart. Electrocardiographic (ECG) ST segment deviations occur within 15-30 seconds after the onset of ischemia [1] and therefore are often used as markers to detect myocardial ischemia. Current literature suggests a transmural progression of ischemia. As the coronary occlusion increases in duration, ischemia progresses uniformly from the subendocardium, which has the highest metabolic demand, to the sub-epicardium and eventually becomes transmural [1].

Results from our animal studies suggest a more complex scenario. We conducted in situ canine experiments simulating demand ischemia by reducing coronary perfusion and increasing the heart rate in a step wise manner through atrial pacing. Epicardial and transmural electrograms were

recorded using a 247 electrode sock and up to 400 transmural needle electrodes. The main finding was that at reduced coronary flow, raising the heart rate caused pockets of ST elevations to appear variously distributed in the epicardial, mid-myocardial and endocardial regions. Further increase in the heart rate, intensified the magnitude and extent of ST elevations, that in certain cases became transmural.

Our findings suggest that the electrographic response of the heart to myocardial ischemia, contrary to earlier belief, is a much more complex phenomenon with hemodynamic and metabolic consequences that help create these conditions. Furthermore, this may impact how we interpret electrical potentials that are measured on the cardiac and body surfaces.

2. Methods

2.1. Experimental preparation

10 mongrel dogs, weighing 23 ± 5 kg, were used to collect data using procedures approved by Institutional Animal Care and Use Committee of the University of Utah and conform to the Guide for the Care and Use of Laboratory Animals (NIH Pub. No. 85-23, Revised 1996). The animals were anesthetized with 30 mg/kg intravenous sodium pentobarbital and ventilated with room air. The heart was exposed through a midsternotomy and suspended in a pericardial cradle. The Left Anterior Descending (LAD) artery was cannulated by making an incision in the dissected segment of the LAD and inserting the cannula. A digital rotary pump was used to draw blood from one of the carotid arteries and control the perfusion rate in the targeted LAD segment. A heat-exchanger setup maintained the blood at physiological temperatures. Periodic monitoring of blood gases ensured adequate ventilation and perfusion so that the pH remained stable throughout the duration of the experiment. Normal coronary perfusion rates and resting heart rates were determined before executing the protocol.

To control heart rate, the right atrium was paced with a bipolar hook electrode. The setup is as shown in Figure 1.



Figure 1. In situ dog heart with 247 electrode sock and 40 transmural needles inserted into the ventricular walls

2.2. Protocol

With control over coronary flow and heart rate, we simulated heart rate stress combined with restricted flow using the following study protocol. At normal perfusion rate, the heart rate was increased step wise, with each step change in heart rate held for 3 minutes. Once all the pre-determined heart rates were cycled through, the heart rate was returned back to normal and the preparation allowed to stabilize for 12 minutes. The heart rate cycle was repeated for a range of perfusion rates. Each successive reduction in perfusion rate was followed by return to normal flow rate and resting heart rate for 12 minutes to allow the animal to stabilize.

2.3. Data acquisition and analysis

Epicardial signals were recorded from both the ventricles using a 247 sock electrode array. The construction of electrode sock is described elsewhere [2]. Up to 40 flexible fiberglass needles [3], each carrying 10 electrodes along its length, were inserted in to the ventricular walls to record transmural signals. The potentials from the sock and needle electrodes were recorded using a customized acquisition system permitting simultaneous recordings of 1024 channels at 1 KHz sampling rate [4]. We used a single lead as remote reference for all unipolar signals. Signal post-processing comprised of gain-adjustment of all channels as well as selecting of single representative beat and doing linear baseline adjustment for each recorded signal. The transmural signals from the 450 needle electrodes were mapped on to a volumetric tetrahedral mesh derived from the anatomical MRI scan of the excised heart [5]. The signals were interpolated using volumetric laplacian

interpolation to reconstruct potentials throughout the volume. Signal analysis was done by cutting planes through the volume and evaluating the potential distribution. The results were visualized in SCIRun [6] as shown in the Results section below.

2.4. Left ventricular segmentation

We use the standardized 17 segment LV model recommended by Cerqueira et.al [7] to identify the locations of ST elevations on the left ventricle (LV). All segments span the full thickness of the LV. Furthermore, we divide each segment along its long axis to create a distribution of 30%, 40%, and 30% for the sub-epicardial (S), mid-myocardial (M) and endocardial (N) regions of the heart as shown in Figure 2 and Table 1.

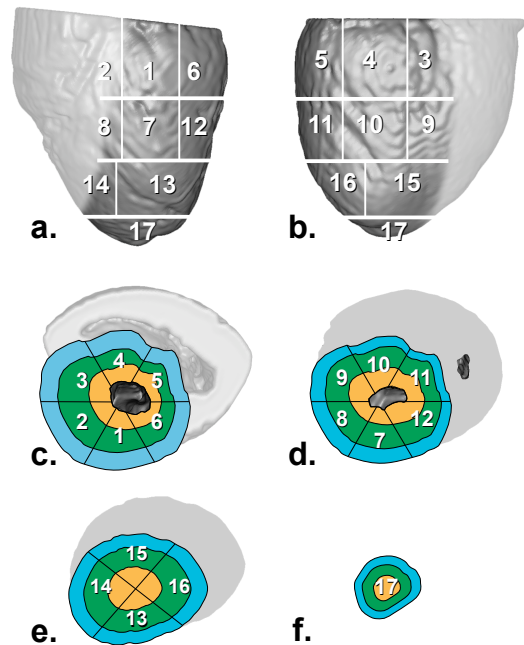


Figure 2. 17 segment Left Ventricle (LV) model. a, LV anterior view. b, LV posterior view. c, Cross section of the basal region. d, Cross section of the mid region. e, Cross section of the apical region. f, Apex cross section. Each segment spans the full thickness of the LV and the differently colored concentric regions represent the outer sub-epicardium (S), mid-myocardium (M) and the inner endocardium (N)

Table 1. Location of 17 segments on the left ventricle

1. basal anterior	10. mid inferior
2. basal anteroseptal	11. mid inferolateral
3. basal inferoseptal	12. mid anterolateral
4. basal inferior	13. apical anterior
5. basal inferolateral	14. apical septal
6. basal anterolateral	15. apical inferior
7. mid anterior	16. apical lateral
8. mid anteroseptal	17. apex
9. mid inferoseptal	

3. Results

Table 2 summarizes the results from our animal studies. We focus here on specific results that illustrate the heterogeneity and complexity of the progression of ST elevated regions.

Table 2. Location of ST elevated regions

Flow Rate (ml/min)	Heart Rate (bpm)	Location
30	142	7M, 7N
30	153	7M, 7N
30	167	7M, 7N
30	182	7M, 7N
30	200	7M, 7N
30	222	7M, 7N
23	142	7M, 7N
23	153	7M, 7N
23	167	7M, 7N
23	182	7M, 7N
23	200	7M, 7N
23	222	7M, 7N
16	142	7M, 7N
16	153	7M, 7N
16	167	7M, 7N
16	182	7M, 7N
16	200	7M, 7N
16	222	7M, 7N
9	153	7M, 7N
9	167	7M, 7N
9	182	7M, 7N, 7S
9	200	7M, 7N, 7S
9	222	7 (Transmural)

When subjected to a slightly reduced flow rate (30 ml/min) and moderately elevated heart rate (182 bpm), pockets of ST elevations are seen developing in segment

7 of the LV model. Specifically, two ST elevated regions in the mid-myocardium (7M) and one in the endocardium (7N) are seen, as shown in Figure 3.

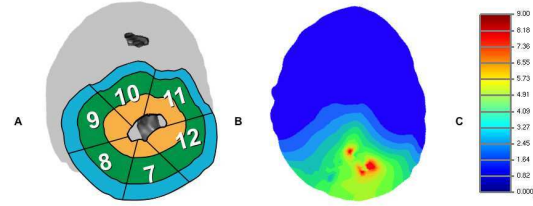


Figure 3. Development of ST elevated regions in 7M and 7N at flow rate of 30 ml/min and heart rate of 182 bpm. **A**, Mid region of the LV segmentation model. **B**, Cross section of the mid region. Two distinct pockets of ST elevations are developing in mid-myocardium and one in the endocardium. **C**, Color scale: 0-9 mV

While maintaining the same elevated heart rate (182 bpm), reducing the flow rate to 23 ml/min increases the magnitude of ST elevated regions as seen in Figure 4, when compared with those seen at 30 ml/min.

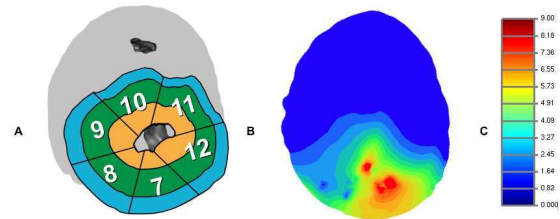


Figure 4. Progression of ST elevated regions in 7M and 7N at flow rate of 23 ml/min and heart rate of 182 bpm. **A**, Mid region of the LV segmentation model. **B**, Cross section of the mid region. ST elevated regions are increasing in magnitude in the endocardial and mid-myocardial regions of segment 7. **C**, Color scale: 0-9 mV

Reducing the flow rate to 16 ml/min, while simultaneously raising the heart rate to 222 bpm results in further expansion of the ST elevated regions. Additionally, the two pockets of ST elevations in the mid-myocardium (7M) merge to form a bigger region of ST elevation as seen in Figure 5.

At extremely low flow rate (9 ml/min) and elevated heart rate (222 bpm) the region becomes transmural. As shown in Figure 6, the pockets of ST elevations in 7M and 7N have merged in to a single transmural region of ST elevation.

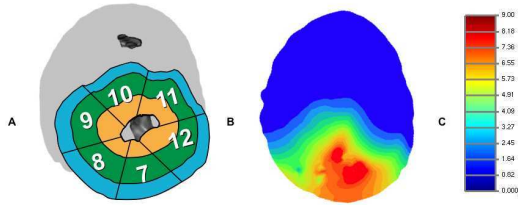


Figure 5. Expansion of ST elevated regions in 7M and 7N at flow rate of 16 ml/min and heart rate of 222 bpm. **A**, Mid region of the LV segmentation model. **B**, Cross section of the mid region. ST elevated regions have further increased in magnitude. In addition, the two pocket of ST elevations in the mid-myocardium (7M) have now merged to form a bigger ST elevated region. **C**, Color scale: 0-9 mV

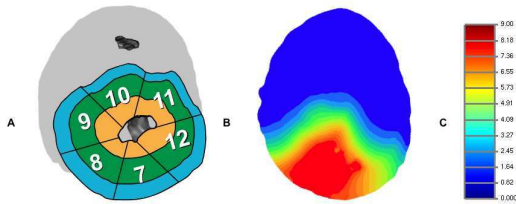


Figure 6. Transmural ST elevation in segment 7 at flow rate of 9 ml/min and heart rate of 222 bpm. **A**, Mid region of the LV segmentation model. **B**, Cross section of the mid region. The pockets of ST elevated regions in the mid-myocardium and the endocardium of segment 7 have merged in to a single transmural ST elevated region. **C**, Color scale: 0-9 mV

4. Discussion and conclusions

Reimer *et al.* and others, have suggested, based on their experiments that the progression of ischemia is transmural, originating from the sub-endocardium and extending uniformly to the sub-epicardium. This class explanation of endocardial and sub-endocardial ischemia has led to simple source models and thus a way to parameterize and interpret ST segment shifts on the body surface. The results presented in this paper show that myocardial ischemia, characterized by ST elevations has a more complex pattern of distribution and progression than previously believed. Pockets of ST elevations occur variously distributed in the mid-myocardial and endocardial regions, when subjected to slightly reduced flow rate and moderately elevated heart rate. Further reduction in coronary flow results in expansion of these ST elevated regions. In addition, some of the ST elevated regions begin to merge to form bigger regions of ST elevations. At extremely low flow rate and high heart rate, the entire region shows transmural ST elevation.

This heterogeneous and complex pattern of progression of the ST elevated regions entails potentially a new set of metabolic and hemodynamic consequences. Furthermore, this may impact how we interpret electrical potentials on the heart and eventually on the body surface, particularly in diagnosing non-transmural ischemia. We plan to further develop and refine our techniques using MRI and CT modalities to accurately capture the fiber orientation and vasculature and examine their influence on the distribution and progression of ST elevations.

Acknowledgements

This work was made possible by grant from Nora Eccles Treadwell foundation as well as software from the NIH/NCRR Center for Integrative Biomedical Computing, P41-RR12553-10.

References

- [1] Reimer K, Jennings R. Myocardial ischemia, hypoxia and infarction. In Fozzard H, et al (eds.), *The Heart and Cardiovascular System*. New York: Raven Press, 1992; 1875–1973.
- [2] Arisi G, Macchi E, Corradi C, Lux R, B. T. Epicardial excitation during ventricular pacing. relative independence of breakthrough sites from excitation sequence in canine right ventricle. *Circ Res* 1992;71:840–849.
- [3] Rogers J, Melnick S, Huang J. Fiberglass needle electrodes for transmural cardiac mapping. *IEEE Trans Biomed Eng* 2002;49:1639–1641.
- [4] Ershler P, Steadman K, Moore K, Lux R. Systems for measuring and tracking electrophysiological distributions: Current tools for clinical and experimental cardiac mapping. *IEEE Trans Biomed Eng* 1998;26:56–61.
- [5] MacLeod RS, Stinstra J, Lew S, et al. Subject-specific, multiscale simulation of electrophysiology: a software pipeline for image-based models and application examples. *Phil Trans R Soc A* 2009;367:2293–2310.
- [6] Parker SG, Johnson CR. Scirun: A scientific programming environment for computational steering. *Supercomputing* 1995;.
- [7] Cerqueira M, Weissman N, Dilsizian V, et al. Standardized myocardial segmentation and nomenclature for tomographic imaging of the heart. *Circulation* 2002;105:539–542.

Address for correspondence:

Kedar Aras

Nora Eccles Harrison Cardiovascular Research and Training Institute, University of Utah

95 South. 2000 East. Salt Lake City, UT 84112

E-mail address (kedar@sci.utah.edu)